

Acoustic impedance measurement using sine sweep excitation and known volume velocity technique

Rajendra Singh

Carlyle Compressor Company, Carrier Corporation, Syracuse, New York 13221

Michael Schary

Research Division, Carrier Corporation, Syracuse, New York 13221

(Received 24 April 1978)

The direct determination of acoustic impedance requires the measurements of both pressure and volume velocity, but the latter in general cannot be measured directly. Thus, other means must be adopted to bypass this measurement problem. This paper presents two methods which utilize excitation of a system with known volume velocity. This, along with measured pressure response, provides both magnitude and phase of impedance as continuous functions of frequency. The first method uses a convertible acoustic horn driver for excitation. Its volume velocity is determined by measuring calibrated pressure in a fixed cavity at the back of the driver. The second method uses for excitation an electrodynamic shaker driven piston which carries an accelerometer. This signal is integrated to yield input acoustic velocity information. The two-channel analog signal processing setup includes the following instruments: sine sweep oscillator, tracking filters, log converters, phase meter, etc. In order to establish the validity of the proposed experimental techniques, several example cases have been evaluated. Excellent agreement between theory and measurements are obtained for driving point and transfer impedances over the plane wave frequency regime. The advantages of the methods proposed here over some other established techniques are as follows: (1) our methods are easier to use, (2) continuous impedance spectra are obtained quickly, (3) excellent dynamic range is achieved, and (4) complications of digital systems are not involved.

PACS numbers: 43.85.Bh

INTRODUCTION

The dynamic nature of fluid machinery manifolds can be characterized by acoustic impedances which, together with source and termination information, allow the prediction of pressure oscillations.¹ In the case of some complicated and irregular geometries often seen in practice, experimental means must be adopted to evaluate the following: (i) eigenvalues for design and noise control purposes, and (ii) both magnitude and phase of driving point (input) and cross point (transfer) impedances to build and/or verify manifold mathematical simulation models.¹

A number of impedance measurement techniques with certain inherent strengths and limitations are available. The standing wave tube method²⁻⁵ is widely accepted but is generally time consuming because of the multiple single-frequency measurements required; also, it is error prone at low frequencies and for small diameter components. Other methods include the "toneburst" pulse method,^{3,5} impulse technique,⁶ two-microphone comparison method,⁵ two-microphone cross-correlation/spectral-density method,⁷ four-pole coefficients measurement,⁸ etc. All of these methods avoid volume velocity measurement, which in general is not feasible. A number of investigators^{9,10} have, however, built constant-volume-velocity sources which reduce the requirements to one pressure response measurement, which is directly proportional to the acoustic impedance magnitude; phase accuracy, however, is questionable. Moreover, because of resonance loading effects, constant excitation may be difficult to maintain. There-

fore, simultaneous measurement of excitation and response is very desirable for impedance measurement, as demonstrated by Singh and Soedel.¹¹ In this study, acoustic excitation is provided by a shaker driven oscillating piston whose motion is monitored by a displacement transducer. Volume or particle velocity measurements have also been attempted for a steady-state single-frequency excitation with hot-wire anemometer,¹² but its calibration and reliability are generally suspect.

A few methods^{6,7,11,12} allow continuous frequency measurements, but these have limited dynamic range, depending upon the type of excitation.¹³ The present method proposes to achieve continuous frequency measurement with an improved dynamic range by using a sinusoidal frequency sweep excitation. Moreover, the technique aims to determine impedances in complex form over the plane wave frequency regime from simultaneous measurement of pressure and volume velocity. Two methods of determining the latter will be presented here.

I. CONVERTIBLE ACOUSTIC DRIVER METHOD

A convertible acoustic horn driver with a throat on each end can be attached to the acoustic system under study at its front end F , and a fixed cavity of volume V can be mounted at its back end B , as shown in Fig. 1. In the fixed cavity, it can be assumed that the cavity pressure p_V is related to the throat volume velocity only through the elastic properties of volume V . However, acoustic driver dynamics and the difference between

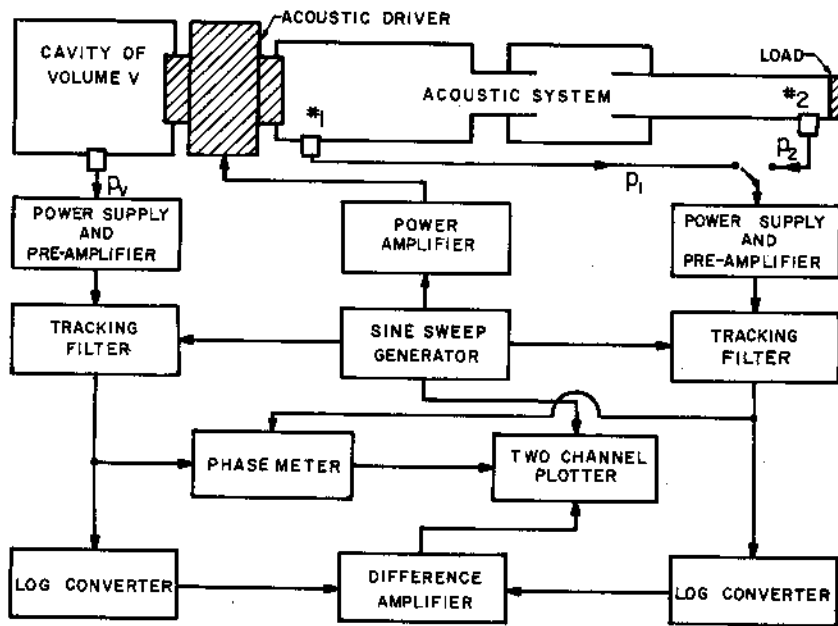


FIG. 1. Schematic of acoustic impedance measurement setup using convertible acoustic driver method: method I. Transfer function plots are adjusted for transducer sensitivities and volume velocity calibration factor $\bar{K}(f)$ to yield impedance spectra.

front and back throat volume velocities Q_F and Q_B should also be considered for calibration.

Input acoustic impedance $\bar{Z}_{11}(f)$ is defined as

$$\bar{Z}_{11}(f) = |Z_{11}(f)| e^{j\psi_{11}(f)} = \bar{p}_1(f) / \bar{Q}_1(f), \tag{1}$$

where \bar{p}_1 is the pressure at driving point (No. 1), \bar{Q}_1 is the input volume velocity, j is the imaginary number, f is excitation frequency, and a tilde over a symbol indicates that it is a complex quantity and possesses both magnitude and phase. \bar{Q}_1 is given as

$$\begin{aligned} \bar{Q}_1(f) &= \bar{Q}_F(f) = \bar{H}_{FB}(f) \bar{Q}_B(f) \\ &= \bar{H}_{FB}(f) (j2\pi fV / \rho c^2) \bar{p}_V(f), \end{aligned} \tag{2}$$

where $\bar{H}_{FB}(f)$ is the transfer function between the front and back ends and can be either computed from driver configuration or measured (present case) by placing identical cavities at each end, ρ is the medium density, and c is the medium sonic speed. From (1) and (2), $\bar{Z}_{11}(f)$ in terms of $\bar{p}_1(f)$ and $\bar{p}_V(f)$ is

$$\bar{Z}_{11}(f) = \bar{K}(f) [\bar{p}_1(f) / \bar{p}_V(f)], \tag{3}$$

where $\bar{K}(f)$ is the volume velocity calibration factor, and is given by

$$\bar{K}(f) = -j\rho c^2 / [2\pi fV \bar{H}_{FB}(f)]. \tag{4}$$

Transfer impedance $\bar{Z}_{12}(f)$, i.e., response at point No. 2 from excitation at No. 1, is similarly given as

$$\bar{Z}_{12}(f) = |Z_{12}(f)| e^{j\psi_{12}(f)} = \bar{K}(f) [\bar{p}_2(f) / \bar{p}_V(f)]. \tag{5}$$

The impedance phase $\psi(f)$ will be presented in degrees from -180° to $+180^\circ$ and magnitude as $20 \log_{10} |Z(f)|$ in dB *re* $4 \times 10^9 \text{Ns/m}^5$.

The steady-state response of a linear acoustic system is harmonic if excited with a sine wave of any frequency. Thus, the acoustic system shown in Fig. 1 can be driven at a fixed frequency by an audio oscillator, and \bar{p}_V and \bar{p}_1 waveforms can be acquired simultaneously

and then compared on a two-channel oscilloscope for relative amplitude (i.e., $|Z|$) and time delay (i.e., ψ). Thus, the complete impedance spectrum can be generated by incrementing excitation frequencies over the range of interest. This single-frequency measurement of course is time consuming, but provides a large dynamic range R . For continuous frequency measurement, the excitation function should contain uniform energy over the frequency range. This can be achieved by impulse, transient, or random excitations (a parallel approach to frequency excitation); however, R is limited by the energy density in the excitation. Sine sweep excitation (a series approach to frequency excitation) on the other hand offers an attractive alternative because at each frequency, a large amount of energy can be input, thus achieving a good signal to noise ratio. However, the sweep rate must be low enough to ensure that the steady-state conditions are sufficiently approached; otherwise, this excitation will resemble transient excitation with limited R .

Figure 1 shows schematically the measurement setup and instrumentation. Two tracking filters, tuned at the frequency of excitation through synchronization with sine sweep generator, produce mutually coherent pressures, $\bar{p}_V(f)$ and $\bar{p}_1(f)$ or $\bar{p}_2(f)$, with good signal to noise ratio. Some of the pertinent dynamic data of the instrumentation shown in Fig. 1 are as follows:

(i) acoustic driver—30 W; (ii) microphones—12-mm diameter, sensitivity = -70 dB (0 dB = 10 V/Pa); (iii) preamplifiers—gain = 20 dB; (iv) sine sweep generator—sweep rate = 10 Hz/s; (v) tracking filters—bandwidth = 10 Hz, filter rolloff slope ≈ 1 dB/Hz. The overall measurement and data processing time is 200 s for a 20–2000-Hz frequency range. The overall accuracy limits are estimated to be as follows:

- (i) magnitude $|Z|$, ± 1 dB
- (ii) phase ψ , $\pm 5^\circ$.

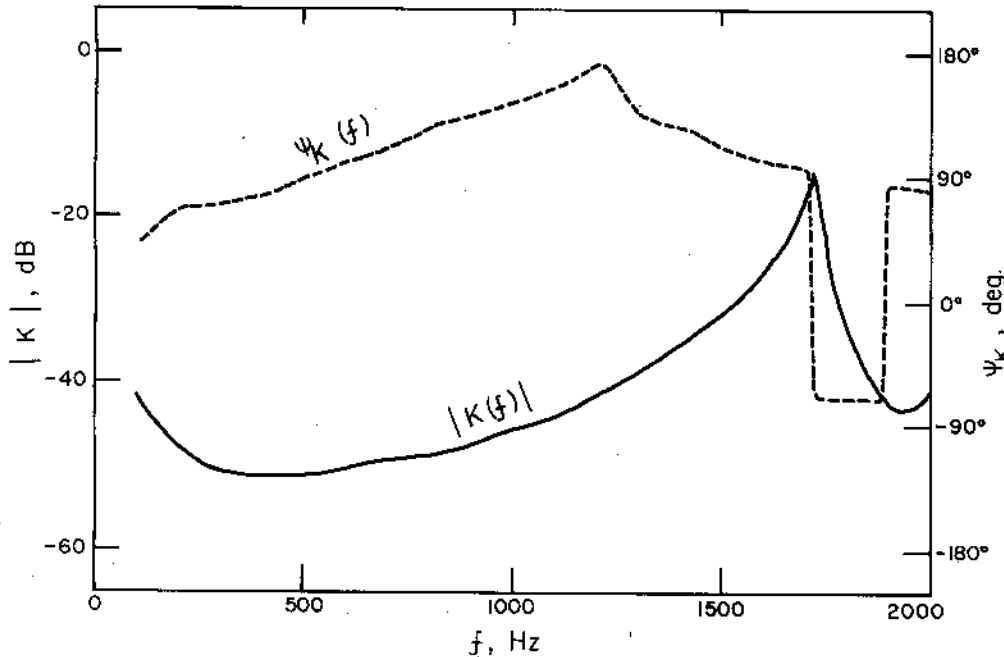


FIG. 2. Volume velocity calibration factor $\bar{K}(f)$.

For the present setup, the volume velocity calibration factor $\bar{K}(f)$, as given by (3), is shown in Fig. 2. The front and back volume velocities not only differ in magnitude but also in phase. At around 1710 Hz, the front volume velocity level drops drastically, which produces a sharp dip in the \bar{p}_1 or \bar{p}_2 measurement. However, since a transfer function is being measured here, the impedance values do not exhibit it.

In order to verify the measurement method, experimental and theoretical¹⁴ (curve constructed from 100 discrete points, 20 Hz apart) results have been compared for a number of example cases. One complete impedance set is presented in Fig. 3 for a circular tube with closed termination. (Note that this boundary condition is not a limitation of the method; in fact, any ideal or realistic boundary condition can be chosen.) The results shown in Fig. 3 show excellent agreement between experiment and theory. The slight shift in higher resonance frequencies is not due to any deficiency in the measurement, rather it demonstrates that the tube lengths used for measurement and computation do differ slightly, which is especially noticeable at higher frequencies. The discussion on the magnitude dynamic range will be covered in a later section.

Figure 4 shows a composite acoustic system which is typical of a discharge manifold for a single cylinder (or dynamically uncoupled twin cylinders). The transfer impedance $\bar{Z}_{12}(f)$ measured spectra are compared to theory in Fig. 5; note the excellent agreement. It should be mentioned that $|Z_{12}(f)|$ is an indication of the transmissibility by this manifold system as high impedance values signify little attenuation.

Although the results have been acquired for air (a) medium at rest, these can be converted to any other medium, say refrigerants (γ) at rest, by using the fol-

lowing transformations:

$$f_\gamma = (c_\gamma/c_a)f_a \quad \text{and} \quad \bar{Z}_\gamma(f_\gamma) = (\rho_\gamma c_\gamma/\rho_a c_a)\bar{Z}_a(f_a). \quad (6)$$

For some refrigerants, such as R-12 and R-22 at room temperature and pressure, an approximate relationship is as follows:

$$f_\gamma \approx 1/2 f_a \quad \text{and} \quad \bar{Z}_\gamma(f_\gamma) \approx 2 \bar{Z}_a(f_a). \quad (7)$$

Thus, as an approximation the frequency scale in Figs. 3 and 5 can be halved and magnitudes increased by 6 dB for obtaining refrigerant medium based impedance spectra.

II. SHAKER-PISTON METHOD

Sound waves in a duct can be generated by placing an oscillating piston at one end. The propagated wave will be a plane wave front if the following ideal conditions are satisfied¹⁴: (i) perfect piston driving surface, (ii) rigid duct walls, and (iii) negligible viscous and thermal boundary dissipations at the wall. Realistically speaking, these conditions do not pose any severe limitations and, in general, plane wave propagation is obtained over a wide frequency range (for example, 20–2000 Hz for a 50-mm-diam tube with air medium for the present study). There is no volume velocity escape through the space between the piston and rigid tube walls as the tightness of the piston (with an o ring) is satisfactory, and the piston moves well even in the absence of any lubrication. However, nonlinear distortion can be induced by either piston wear or misalignment.

The present measurement setup differs from the Singh and Soedel investigation¹¹ in the following manner. (i) The present technique utilizes a different type of excitation. (ii) The piston velocity is obtained presently by integrating a signal from an accelerometer mounted

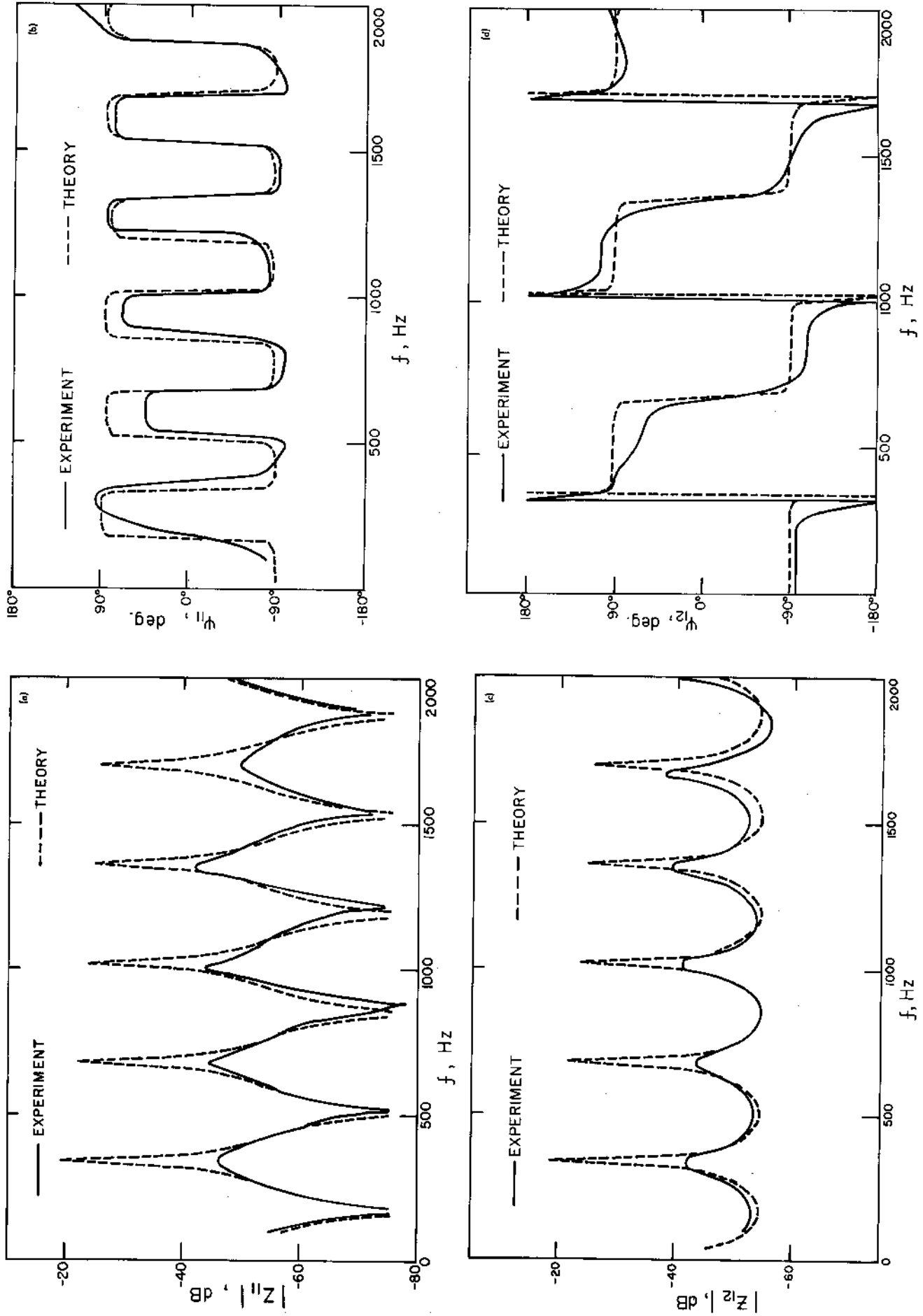


FIG. 3. Impedance spectra for a closed tube of length 508 mm and diameter 25 mm using method I for (a) input impedance magnitude $|Z_{11}(f)|$, (b) input impedance phase $\psi_{11}(f)$, (c) transfer impedance magnitude $|Z_{12}(f)|$, and (d) transfer impedance phase $\psi_{12}(f)$. Medium: air.

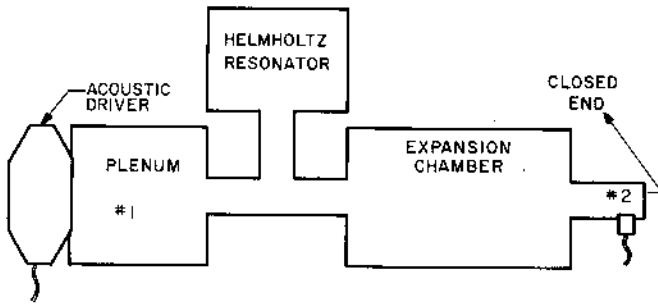


FIG. 4. Schematic of a positive displacement compressor manifold. The cylinder and valves are at the plenum inlet where acoustic driver is placed for impedance measurement. The boundary condition at the muffler outlet has been chosen to be a closed termination for measurement convenience; in reality, the boundary condition is probably anechoic, which is difficult to construct, especially at low frequencies.

on the piston; this has two advantages over the displacement transducer detection used previously¹¹—(a) easier calibration and (b) signal integration is easier than differentiation. (iii) The present setup uses analog data acquisition and processing techniques, which do not involve the complications of digital systems used by Singh and Soedel.¹¹ It is interesting to note here that the sine sweep excitation method with digital signal processing techniques is more complicated.

Figure 6 shows schematically the measurement setup and instrumentation. Some of the pertinent dynamic data are as follows: (i) electrodynamic shaker—force = 18N rms; (ii) accelerometer—sensitivity = 3.36 pC/g, weight = 2.5 g, diameter ≈ 7 mm, and height ≈ 12 mm; and (iii) other instrumentation the same as listed in Sec. I.

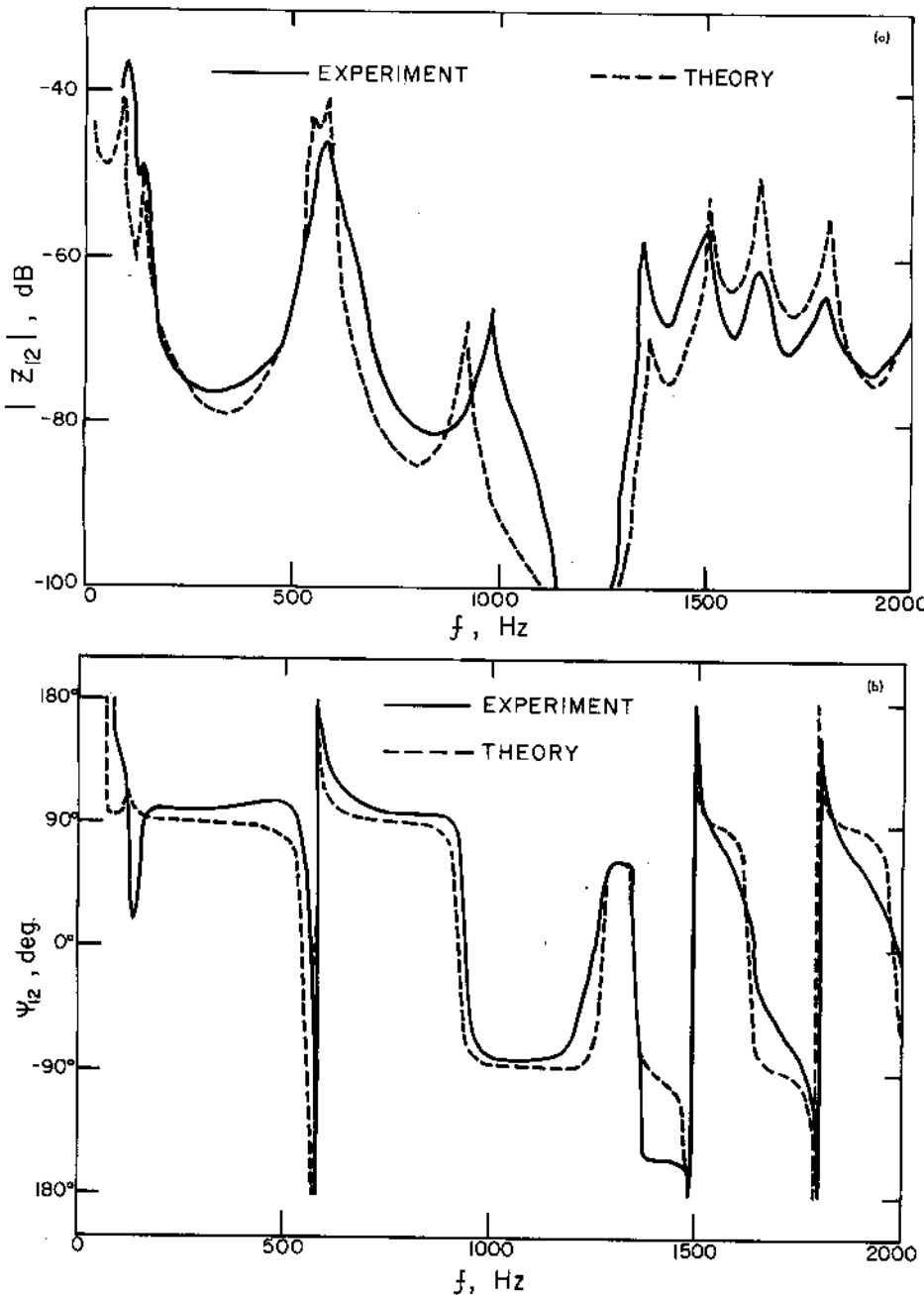


FIG. 5. Impedance spectra for manifold shown in Fig. 4 using method I for (a) transfer impedance magnitude $|Z_{12}(f)|$, and (b) transfer impedance phase $\psi_{12}(f)$. Medium: air.

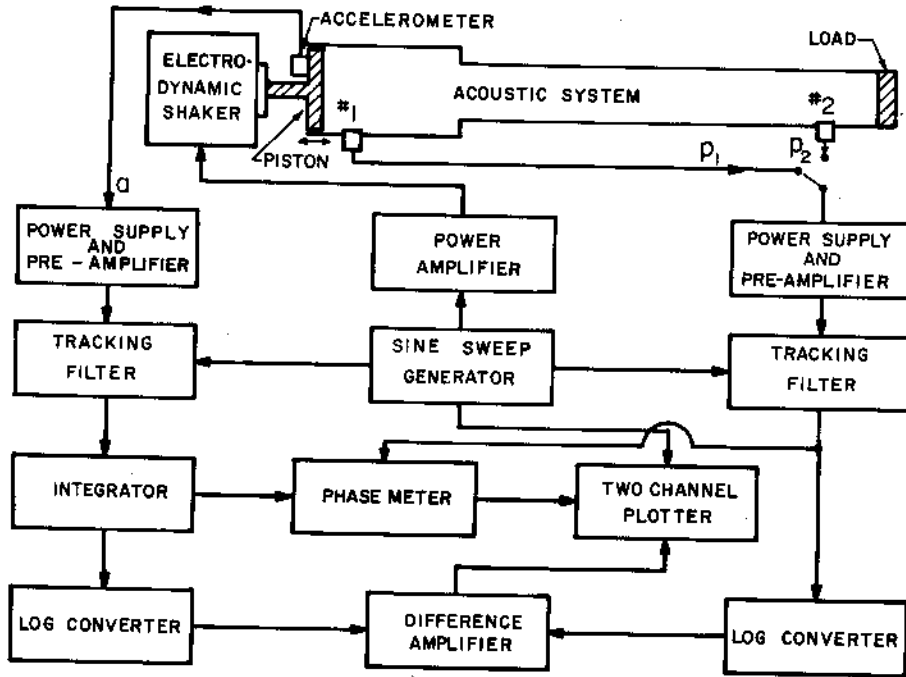


FIG. 6. Schematic of acoustic impedance measurement setup using shaker-piston method, method II. Transfer function plots are adjusted for transducer sensitivities to yield impedance spectra.

The input volume velocity $\bar{Q}_1(f)$ is

$$\bar{Q}_1(f) = S_1 \bar{v}(f) = -j S_1 \bar{a}(f) / 2\pi f, \tag{8}$$

where S_1 is the cross-sectional area at the driving point (No. 1) and a is the piston acceleration whose integration [expressed in (8) for harmonic signals] yields piston velocity v , which should be equal to the acoustic particle velocity at the driving point. Figure 7 shows piston acceleration and velocity spectra for the present setup. Although the piston displacement is extremely low (0.0035-mm peak to peak at 320 Hz), the velocity level is sufficient to create acoustic pressures with good signal-to-noise ratio.

Input and transfer impedances $\bar{Z}_{11}(f)$ and $\bar{Z}_{12}(f)$ are

$$\bar{Z}_{11}(f) = |Z_{11}(f)| e^{j\theta_{11}(f)} = \bar{p}_1(f) / S_1 \bar{v}(f) = j 2\pi f \bar{p}_1(f) / S_1 \bar{a}(f), \tag{9a}$$

$$\bar{Z}_{12}(f) = |Z_{12}(f)| e^{j\theta_{12}(f)} = \bar{p}_2(f) / S_1 \bar{v}(f)$$

$$= j 2\pi f \bar{p}_2(f) / S_1 \bar{a}(f). \tag{9b}$$

Results obtained by the shaker-piston method are compared with theory in Fig. 8 for a closed tube; note the excellent agreement for both magnitude and phase.

III. COMPARISON OF DYNAMIC RANGE

Measurement dynamic range R depends upon the following: (i) frictional characteristics of the acoustic system under study, (ii) type of excitation, (iii) type of exciter, (iv) transducer sensitivity and preamplification, (v) dynamics of the detection and analysis instrumentation, and (vi) ambient and instrumentation noise levels.

Table I compares the methods presented here for R , based upon the acoustic impedance of a circular tube with closed and open terminations. These are also compared with theory which includes frequency-depen-

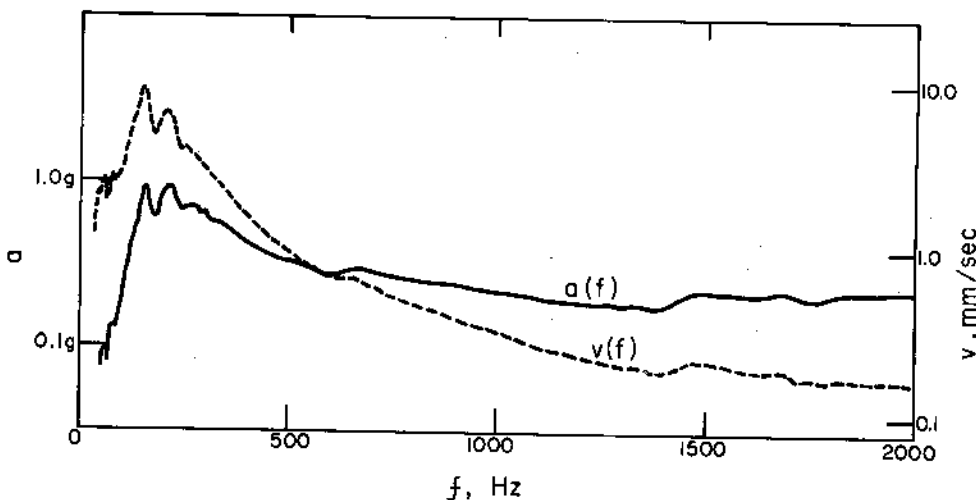


FIG. 7. Piston acceleration a and velocity v spectra.

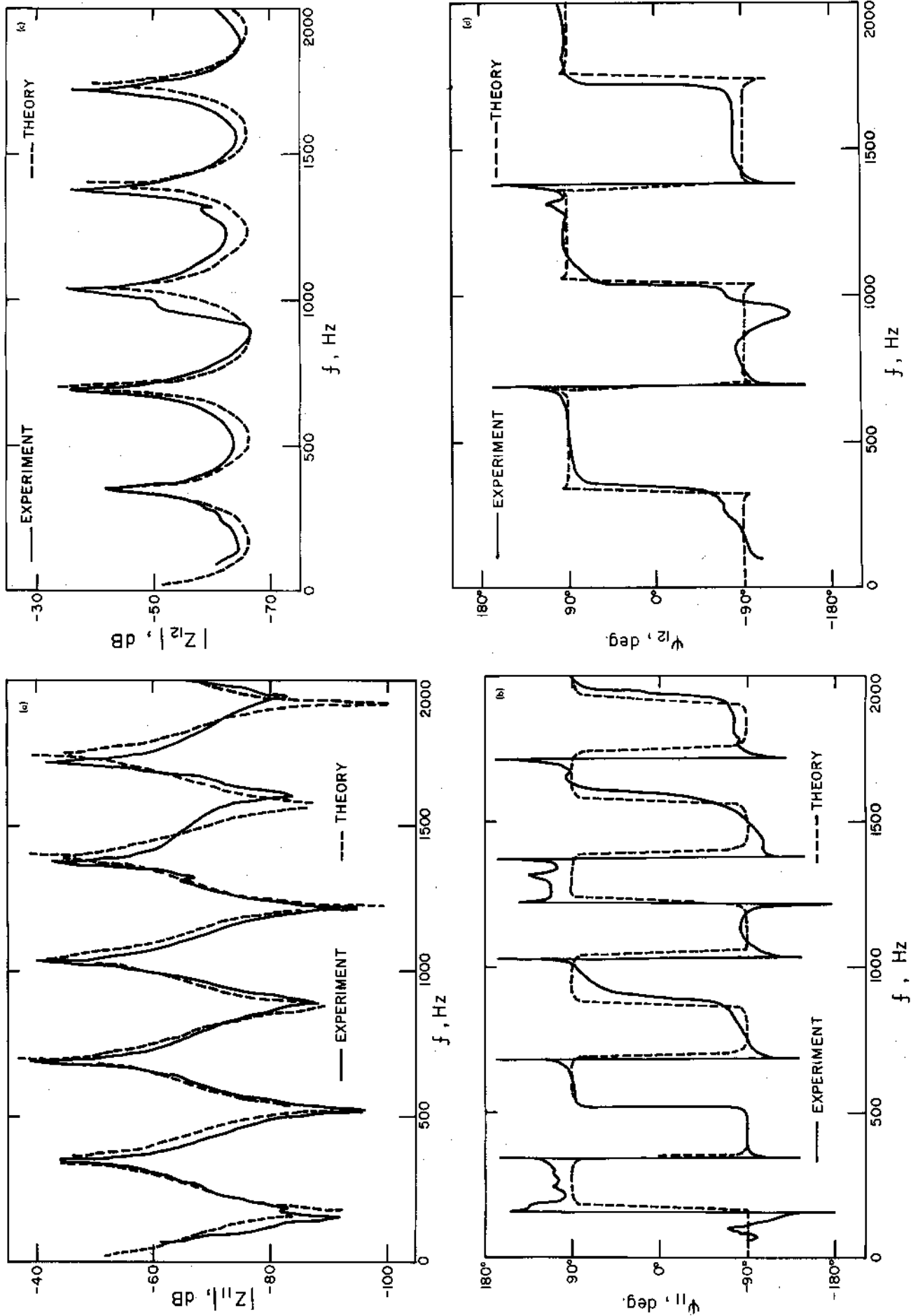


FIG. 8. Impedance spectra for a closed tube of length 495 mm and diameter 50 mm using method II, for (a) input impedance magnitude $|Z_{11}(f)|$, (b) input impedance phase $\psi_{11}(f)$, (c) transfer impedance magnitude $|Z_{12}(f)|$, and (d) transfer impedance phase $\psi_{12}(f)$. Medium: air.

TABLE I. Comparison of present method for approximate measurement dynamic range R and damping coefficient ζ , based upon the example case of a circular tube,

Method: theory/experiment	R , dB		ζ	
	$ Z_{11} $	$ Z_{12} $	Low frequency (350–450 Hz)	High frequency (1400–1800 Hz)
(1) Theory (with viscous and thermal boundary dissipations)	65	35	0.004	0.008
(2) Minimum possible experimental values based upon sine sweep rate (10 Hz/s)			0.005	0.001
(3) Measurement method I: convertible acoustic driver method	35	20	0.090	0.015
(4) Measurement method II: shaker-piston method	55	30	0.020	0.008

dent viscous and thermal dissipations at the rigid walls of the tube containing air at rest.¹⁴ Note that the theory serves only as a benchmark and a basis for comparison. Method II provides a higher R than method I and almost approaches the theoretically computed values. The two methods differ in excitation sources, transducers, and preamplifiers; however, usage of high sensitivity microphones in method I did not show any improvement in R . The loss in dynamic range is probably due to the resonance loading of the diaphragm in method I, which should not affect piston motion in method II. Although method I provides a maximum value of R as 35 dB for a circular tube, R equal to 60 dB has been obtained for a composite acoustic system (Fig. 4).

Approximate damping coefficient ζ values are also compared for two frequency regimes in Table I. (ζ is computed from $\zeta = \Delta f_n / 2f_n$, where f_n is the natural frequency and Δf_n is the half-power bandwidth at that frequency.) Also compared in Table I are minimum possible ζ values based upon the sine sweep rate.¹³ Since the actual system damping increases and damping measurement accuracy is improved at higher frequencies, a better correlation between measured and realistic ζ are obtained. As shown in Table I, method I does not

provide ζ as accurate as method II. Note that ζ can also be obtained (probably more accurately) from a phase spectrum.

Table II compares dynamic range as obtained by various continuous frequency type methods employing different excitations. These values represent transmission characteristics such as transfer impedance and have been taken from the published literature. It should be pointed out that it is conceivable to obtain different R for cases other than the example presented. Therefore, Table II is intended to establish a rough order of magnitude comparison. The method presented in this paper provides much better R than any other method listed. Moreover, it compares very favorably with the single-frequency-point measurement methods as well. (For example; $R = 60$ dB with single sine excitation for the second case¹¹ in Table II.)

IV. CONCLUSIONS

This paper has presented two different methods of measuring input volume velocity. This, along with measured pressure response for a sine sweep excitation, is used to determine continuous acoustic imped-

TABLE II. Comparison of continuous frequency type acoustic impedance measurement methods for approximate dynamic range R .

Measurement method	Example case	R , dB
(1) Present method: convertible acoustic driver method	Single-cylinder compressor manifold and muffling system	60
(2) Oscillating piston method (with digital signal processing techniques) ¹¹	Two-cylinder compressor discharge manifold and muffling system	
(i) random (white-noise) excitation		20
(ii) transient (tone-burst) excitation		20
(3) Two-microphone spectral density/random excitation method ⁷	Automobile muffler	22
(4) Impulse excitation method ⁸	Compressor muffler	30
(5) Hot-wire anemometer-sine-increment excitation method ¹²	Brass instrument	40–55

ance magnitude and phase spectra. Conceptually, similar techniques are currently in practice for structural dynamic systems, but the limitation of volume velocity measurement has always been the major roadblock for acoustical systems.

The shaker-piston method not only provides more dynamic range than the convertible acoustic driver method, but also has no inherent low-frequency limitation. Conversely, the convertible acoustic driver method is easier to calibrate and use.

The authors are not aware of any previous similar effort and feel that the methods presented in this paper offer the following advantages over some other established measurement techniques.²⁻¹² (1) Direct measurement of acoustic impedance has been accomplished. (2) Continuous frequency spectrum is obtained rapidly and efficiently, which results in considerable time saving; the overall measurement time is comparable to other continuous frequency type techniques.^{6,7,11,12} (3) Excellent dynamic range is achieved, a significant improvement over other measurement methods^{6,7,11}; note that in the present method signal-to-noise ratio is extremely good (except at antiresonances) and unlike some other techniques,^{6,7,11} no averaging is needed. (4) Unlike the standing wave tube²⁻⁵ and pulse^{3,5} methods, the present methods (except the convertible acoustic driver method below cutoff frequency) do not pose any low-frequency measurement problems. (5) It does not require any complicated measurement setup such as careful transducer locations,⁶ probe microphone and traversing system,² and extremely long measurement tubes,³ etc. (6) Data acquisition and processing procedures are simple and do not require the complications and sophistication of digital signal processing techniques.^{6,7,11}

The major shortcoming may be the resonance loading of the excitation source (especially in the convertible acoustic driver method). This can be corrected by incorporating a feedback loop system.

The authors feel that the present method can also be used to determine fundamental dynamic properties of source and load terminations. This, along with measurements in the presence of fluid flow are currently being investigated.

ACKNOWLEDGMENT

The authors thank P. K. Baade for motivation and J. E. McManus for help.

- ¹R. Singh, E. Sandgren, K. Ragsdell, and W. Soedel, "Simulation of a Two Cylinder Compressor for Discharge Gas Pressure Oscillation Prediction," Am. Soc. Mech. Eng., Paper No. 76-WA/FE-10 (1976).
- ²Am. Soc. Test. Mater., ASTM C384-58, "Impedance and Absorption of Acoustical Materials by the Tube Method," (1975).
- ³W. S. Gatley and R. Cohen, "Methods for Evaluating the Performance of Small Acoustic Filters," J. Acoust. Soc. Am. **46**, 6-16 (1969).
- ⁴T. H. Melling, "An Impedance Tube for Precision Measurement of Acoustic Impedance and Insertion Loss at High Sound Pressure Levels," J. Sound Vib. **28**, 23-54 (1973).
- ⁵K. U. Ingard and V. K. Singhal, "Upstream and Downstream Sound Radiation into a Moving Fluid," J. Acoust. Soc. Am. **54**, 1343-1346 (1973).
- ⁶R. Singh and T. Katra, "Development of an Impulse Technique for Measurement of Muffler Characteristics," J. Sound Vib. **56**, 279-298 (1978).
- ⁷A. F. Seybert and D. F. Ross, "Experimental Determination of Acoustic Properties Using a Two-Microphone Random-Excitation Technique," J. Acoust. Soc. Am. **61**, 1362-1370 (1977).
- ⁸T. Miwa and J. Igarashi, "Fundamentals of Acoustic Silencers (II)—Determination of Four Terminal Constants of Acoustic Elements," Aeronaut. Res. Inst., Rep. 344, 25, Univ. Tokyo (1959).
- ⁹T. Salava, "Sources of Constant Volume Velocity and Their Use for Acoustic Measurements," J. Audio Eng. Soc. **22**, 145-153 (1974).
- ¹⁰J. Merhaut, "Method of Measuring the Acoustical Impedance," J. Acoust. Soc. Am. **45**, 331 (1969).
- ¹¹R. Singh and W. Soedel, "An Efficient Method of Measuring Impedances of Fluid Machinery Manifolds," J. Sound Vib. **56**, 105-125 (1978).
- ¹²R. L. Pratt, S. J. Elliot, and J. M. Bowsher, "The Measurement of Acoustic Impedance of Brass Instruments," *Acustica* **38**, 236-246 (1977).
- ¹³J. T. Broch, "On the Measurement of Frequency Response Function," B & K Tech. Rev. **4**, 3-31 (1975).
- ¹⁴S. N. Rachevkin, *A Course of Lectures on the Theory of Sound* (MacMillan, New York, 1963), Chaps. V and VII.